

# Sampling on Graphs: From Theory to Applications

Yuichi Tanaka, Yonina C. Eldar, Antonio Ortega, and Gene Cheung

## Abstract

The study of sampling signals on graphs, with the goal of building an analog of sampling for standard signals in the time and spatial domains, has attracted considerable attention recently. Beyond adding to the growing theory on graph signal processing (GSP), sampling on graphs has various promising applications. In this article, we review current progress on sampling over graphs focusing on theory and potential applications. Most methodologies used in graph signal sampling are designed to parallel those used in sampling for standard signals, however, sampling theory for graph signals significantly differs from that for Shannon–Nyquist and shift invariant signals. This is due in part to the fact that the definitions of several important properties, such as shift invariance and bandlimitedness, are different in GSP systems. Throughout, we discuss similarities and differences between standard and graph sampling and highlight open problems and challenges.

## I. INTRODUCTION

Sampling—a process producing a discrete-time signal from a continuous-time one—is one of the fundamental tenets of digital signal processing (see [1] and references therein). As such, it has been studied extensively for decades and continues to draw considerable research efforts. Standard sampling theory relies on concepts of frequency domain analysis, shift invariant (SI) signals, and bandlimitedness [2]. This article provides a comprehensive overview of the theory and algorithms for sampling of signals defined on graph domains, i.e., *graph signals*. *Graph signal processing* (GSP) [3], [4]—a fast developing field in the signal processing community—generalizes key signal processing ideas for signals defined on regular domains to discrete-time signals defined over irregular domains described abstractly by graphs. GSP has found numerous promising applications across many engineering disciplines, including image processing, wireless communications, machine learning, and data mining [3]–[6].

Generalization of the sampling problem to GSP raises a number of challenges. First, for a given graph and graph operator the notion of frequency for graph signals is mathematically straightforward, but the connection of these frequencies to actual properties of signals of interest (and thus the practical meaning of concepts such as bandlimitedness and smoothness) is still being investigated. Second, periodic sampling, widely used in traditional signal processing, is not applicable in the graph domain (e.g., it is unclear how to select “every other” sample) and choosing an appropriate sampling set that can adapt to local graph topology is non-trivial. Third, work to date has mostly focused on direct node-wise sampling, while there has been only limited work on developing more advanced forms of sampling, e.g., adapting SI sampling [1] to the graph setting [7], [8]. Finally, graph signal sampling and reconstruction algorithms must be implemented efficiently to achieve a good trade-off between accuracy and complexity.

To address these challenges, various graph sampling approaches have recently been developed, e.g., [9]–[16], based on different notions of graph frequency, bandlimitedness, and shift invariance. For example, a common approach to define the graph frequency is based on the spectral decomposition of different variation operators such as the adjacency matrix or variants of graph Laplacians. The proposed reconstruction procedures in the literature differ in their objective functions leading to a

Y. Tanaka is with the Department of Electrical Engineering and Computer Science, Tokyo University of Agriculture and Technology, Koganei, Tokyo 184–8588, Japan. Y. Tanaka is also with PRESTO, Japan Science and Technology Agency, Kawaguchi, Saitama 332–0012, Japan (email: ytnk@cc.tuat.ac.jp).

Y. C. Eldar is with Faculty of Mathematics and Computer Science, The Weizmann Institute of Science, Rehovot 7610001, Israel (email: yonina.eldar@weizmann.ac.il).

A. Ortega is with the Department of Electrical and Computer Engineering, University of Southern California, Los Angeles, CA 90089 USA (email: antonio.ortega@siipi.usc.edu).

G. Cheung is with the Department of Electrical Engineering and Computer Science, York University, Toronto, M3J 1P3, Canada (email: genec@yorku.ca).

trade-off between accuracy and complexity. A recent review of graph signal sampling [17] mainly focuses on the bandlimited setting, while here we also survey more general graph signal models beyond the bandlimited case. Our goal is to provide a broad overview of existing techniques, highlighting what is known to date in order to inspire further research on sampling over graphs and its use in a broad class of applications in signal processing and machine learning.

The remainder of this paper is organized as follows. Section II reviews basic concepts in GSP and sampling in Hilbert spaces. Graph sampling theory is introduced in Section III along with the sampling-then-recovery framework which is common throughout the paper. Sampling set selection methods are classified and summarized in Section IV where we also introduce fast selection and reconstruction techniques. Applications utilizing graph sampling theory are introduced in Section V. Finally, Section VI concludes this paper with remarks on open problems.

Throughout the paper, we use boldfaced lower-case (upper-case) symbols represent vectors (matrices), the  $i$ th element in a vector  $\mathbf{x}$  is  $x[i]$  or  $x_i$ , and the  $i$ th row,  $j$ th column of a matrix  $\mathbf{X}$  is given by  $[\mathbf{X}]_{ij}$ . A subvector of  $\mathbf{x}$  is denoted as  $\mathbf{x}_{\mathcal{S}}$  with its indicator index set  $\mathcal{S}$ . Similarly, a submatrix of  $\mathbf{X} \in \mathbb{R}^{N \times M}$  is denoted as  $\mathbf{X}_{\mathcal{RC}} \in \mathbb{R}^{|\mathcal{R}| \times |\mathcal{C}|}$ , where indicator indices of its rows and columns are given by  $\mathcal{R}$  and  $\mathcal{C}$ , respectively;  $\mathbf{X}_{\mathcal{RC}}$  is simply written as  $\mathbf{X}_{\mathcal{R}}$ .

## II. REVIEW: GSP AND STANDARD SAMPLING

### A. Basics of GSP

We denote  $\mathcal{G} = (\mathcal{V}, \mathcal{E})$  a graph, where  $\mathcal{V}$  and  $\mathcal{E}$  denote sets of vertices and edges, respectively. The number of vertices is  $N = |\mathcal{V}|$  unless otherwise specified. We define an adjacency matrix  $\mathbf{A}$ , where entry  $[\mathbf{A}]_{mn}$  represents the weight of the edge between vertices  $m$  and  $n$ ;  $[\mathbf{A}]_{mn} = 0$  for unconnected vertices. The degree matrix  $\mathbf{D}$  is diagonal, with  $m$ th diagonal element  $[\mathbf{D}]_{mm} = \sum_n [\mathbf{A}]_{mn}$ . In this paper, we consider undirected graphs without self-loops, i.e.,  $[\mathbf{A}]_{mn} = [\mathbf{A}]_{nm}$  and  $[\mathbf{A}]_{nn} = 0$  for all  $m$  and  $n$ , but most theory and methods discussed can be extended to signals on directed graphs.

GSP uses different variation operators [3], [4] depending on the application and assumed signal and/or network models. Here, for concreteness, we focus on the graph Laplacian  $\mathbf{L} := \mathbf{D} - \mathbf{A}$  or its symmetrically normalized version  $\underline{\mathbf{L}} := \mathbf{D}^{-1/2} \mathbf{L} \mathbf{D}^{-1/2}$ . The extension to other variation operators (e.g., adjacency matrix) is possible with a proper modification of the basic operations discussed in this section. Because  $\mathbf{L}$  is a real symmetric matrix, it always possesses an eigen-decomposition  $\mathbf{L} = \mathbf{U} \mathbf{\Lambda} \mathbf{U}^\top$ , where  $\mathbf{U} = [\mathbf{u}_1, \dots, \mathbf{u}_N]$  is an orthonormal matrix containing the eigenvectors  $\mathbf{u}_i$ , and  $\mathbf{\Lambda} = \text{diag}(\lambda_1, \dots, \lambda_N)$  consists of the eigenvalues  $\lambda_i$ . We refer to  $\lambda_i$  as the *graph frequency*.

A graph signal  $x : \mathcal{V} \rightarrow \mathbb{R}$  is a function that assigns a value to each node. Graph signals can be written as vectors  $\mathbf{x}$ , in which the  $n$ th element,  $x[n]$ , represents the signal value at the  $n$ th node. Note that any vertex labeling can be used, since a change in labeling simply results in row / column permutation of the various matrices, their corresponding eigenvectors and the vectors representing graph signals. The graph Fourier transform (GFT) is defined as

$$\hat{x}[i] = \langle \mathbf{u}_i, \mathbf{x} \rangle = \sum_{n=0}^{N-1} u_i[n] x[n]. \quad (1)$$

Other GFT definitions, e.g., [18]–[21], can also be used without changing the framework. In this article, for simplicity we assume real-valued signals. Although the GFT basis are real-valued for undirected graphs, extensions to complex-valued GSP systems are straightforward.

A *linear graph filter* is defined by  $\mathbf{G} \in \mathbb{R}^{N \times N}$ , which applied to  $\mathbf{x}$  produces an output

$$\mathbf{y} = \mathbf{G} \mathbf{x}. \quad (2)$$

Vertex and frequency domain graph filter designs considered in the literature both lead to filters  $\mathbf{G}$  that depend on the structure of the graph  $\mathcal{G}$ . *Vertex domain filters* are defined as polynomials of the variation operator, i.e.,

$$\mathbf{y} = \mathbf{G} \mathbf{x} = \left( \sum_{p=0}^P c_p \mathbf{L}^p \right) \mathbf{x}, \quad (3)$$

where the output at each vertex is a linear combination of signal values in its  $P$ -hop neighborhood. In *frequency domain filter* design,  $\mathbf{G}$  is chosen to be diagonalized by  $\mathbf{U}$  so that:

$$\mathbf{y} = \mathbf{G}\mathbf{x} = \mathbf{U}\hat{\mathbf{g}}(\mathbf{\Lambda})\mathbf{U}^\top \mathbf{x}, \quad (4)$$

where  $\hat{\mathbf{g}}(\mathbf{\Lambda}) := \text{diag}(\hat{g}(\lambda_1), \dots, \hat{g}(\lambda_N))$  is the graph frequency response. Filtering via (4) is analogous to filtering in the Fourier domain for conventional signals. If there exist repeated eigenvalues  $\lambda_i = \lambda_j$ , then their graph frequency responses must be the same, i.e.,  $\hat{g}(\lambda_i) = \hat{g}(\lambda_j)$ . If  $\hat{g}(\lambda_i)$  is a  $P$ th order polynomial, (4) coincides with vertex domain filtering (3).

### B. Generalized Sampling in Hilbert Space

We next briefly review generalized sampling in Hilbert spaces [1] (see Fig. 1(a)). Let  $x$  be a vector in a Hilbert space  $\mathcal{H}$  and  $c[n]$  be its  $n$ th sample,  $c[n] = \langle s_n, x \rangle$ , where  $\{s_n\}$  is a Riesz basis and  $\langle \cdot, \cdot \rangle$  is an inner product. Denoting by  $S$  the set transformation corresponding to  $\{s_n\}$ , we can write the samples as  $c = S^*x$ , where  $\cdot^*$  represents the adjoint. The subspace generated by  $\{s_n\}$  is denoted by  $\mathcal{S}$ . In the SI setting,  $s_n = s(t - nT)$  for a real function  $s(t)$  and a given period  $T$ . The samples can then be expressed as

$$c[n] = \langle s(t - nT), x(t) \rangle = x(t) * s(-t)|_{t=nT}, \quad (5)$$

where  $*$  is the convolution. The continuous-time Fourier transform (CTFT) of  $c[n]$ ,  $C(\omega)$ , can be written as

$$C(\omega) = R_{SX}(\omega), \quad (6)$$

where

$$R_{SX}(\omega) := \frac{1}{T} \sum_{k=-\infty}^{\infty} S^* \left( \frac{\omega - 2\pi k}{T} \right) X \left( \frac{\omega - 2\pi k}{T} \right) \quad (7)$$

is the sampled cross correlation. Thus, we may view sampling in the Fourier domain as multiplying the input spectrum by the filter's frequency response and subsequently aliasing the result with uniform intervals that depend on the sampling period. In bandlimited sampling,  $s(-t) = \text{sinc}(t/T)$ , where  $\text{sinc}(t) = \sin(\pi t)/(\pi t)$ , while  $s(t)$  can be chosen more generally in the generalized sampling framework.

The recovery of the sampled signal  $c$  is represented as

$$\tilde{x} = WHc = WH(S^*x), \quad (8)$$

where  $W$  is a set transformation corresponding to a basis  $\{w_n\}$  for the reconstruction space, which spans a closed subspace  $\mathcal{W}$  of  $\mathcal{H}$ . The transform  $H$  is called the *correction transformation* and operates on the samples  $c$  prior to recovery. The reconstruction problem is to choose  $H$  so that  $\tilde{x}$  is either equal to  $x$ , or as close as possible under a desired metric. Typically, solving this problem requires making assumptions about  $x$ , e.g., that it lies in a known subspace or is smooth.

In the SI setting, the recovery corresponding to (8) is given by

$$\tilde{x}(t) = \sum_{n \in \mathbb{Z}} (h[n] * c[n])w(t - nT), \quad (9)$$

where a discrete-time correction filter  $h[n]$  is first applied to  $c[n]$ : The output  $d[n] = h[n] * c[n]$  is interpolated by  $w(t - nT)$ , to produce the recovery  $\tilde{x}(t)$ .

Suppose that  $x$  lies in an arbitrary subspace  $\mathcal{A}$  of  $\mathcal{H}$  and assume that  $\mathcal{A}$  is known. Hence,  $x$  can be represented as

$$x = \sum d[n]a_n = Ad, \quad (10)$$

where  $\{a_n\}$  is an orthonormal basis for  $\mathcal{A}$  and  $d[n]$  are the expansion coefficients of  $x$ . In the SI setting,  $x(t)$  is written as

$$x(t) = \sum_{n \in \mathbb{Z}} d[n]a(t - nT), \quad (11)$$

for some sequence  $d[n]$  where  $a(t)$  is a real generator satisfying the Riesz condition. In the Fourier domain, (11) becomes

$$X(\omega) = D(e^{j\omega T})A(\omega), \quad (12)$$

where  $A(\omega)$  is the CTFT of  $a(t)$  and  $D(e^{j\omega T})$  is the discrete-time Fourier transform of  $d[n]$ , and is  $2\pi/T$  periodic.

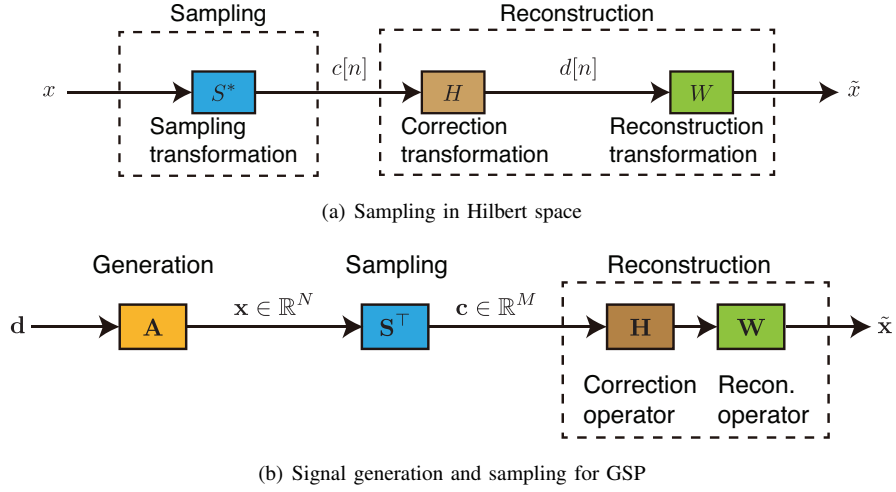


Fig. 1: Generalized sampling frameworks for sampling in Hilbert space and its GSP counterpart.

In this article, we focus on generalized sampling for the unconstrained case, where an arbitrary transformation can be used as  $W$ . We can also consider generalized sampling for a predefined  $W$  ([1], [22] and references therein). In the unconstrained setting, we may recover a signal in  $\mathcal{A}$  by choosing  $W = A$  in (8). If  $S^*A$  is invertible, then perfect recovery of any  $x \in \mathcal{A}$  is possible by using  $H = (S^*A)^{-1}$ . Invertibility can be ensured by the direct-sum (DS) condition:  $\mathcal{A}$  and  $\mathcal{S}^\perp$  intersect only at the origin and span  $\mathcal{H}$  jointly so that

$$\mathcal{H} = \mathcal{A} \oplus \mathcal{S}^\perp. \quad (13)$$

Under the DS condition, a unique recovery is obtained by an oblique projection operator onto  $\mathcal{A}$  along  $\mathcal{S}^\perp$  given by

$$\tilde{x} = A(S^*A)^{-1}S^*x = x. \quad (14)$$

In the SI setting, the frequency response of the correction filter is

$$H(\omega) = \frac{1}{R_{SA}(\omega)}, \quad (15)$$

where  $R_{SA}(\omega)$  is given by (7).

If  $\mathcal{A}$  and  $\mathcal{S}^\perp$  intersect, then there is more than one signal in  $\mathcal{A}$  that matches the sampled signal  $c$ . We may then consider several selection criteria to obtain an appropriate signal out of (infinitely) many candidates. Here, we consider the least squares (LS) approach, but other methods, e.g., based on the minimax criterion, can be used as well [1]. The LS recovery is the minimum energy solution

$$\tilde{x} = \arg \min_{x \in \mathcal{A}, S^*x=c} \|x\|^2, \quad (16)$$

and is given by

$$\tilde{x} = A(S^*A)^\dagger S^*x. \quad (17)$$

Here,  $H = (S^*A)^\dagger$  and  $\cdot^\dagger$  represents the Moore-Penrose pseudo inverse. Its corresponding form in the SI setting is the same as (15), but  $H(\omega) = 0$  if  $R_{SA}(\omega) = 0$ .

### III. GRAPH SAMPLING THEORY

In this section, we first describe a general graph signal sampling and reconstruction framework that is inspired from that of Section II-B. Then, we discuss graph signal models and two definitions of graph signal sampling. Finally, we present recovery experiments both for bandlimited and full-band signals.

### A. General sampling and recovery framework

We consider finite dimensional graphs and graph signals for which the generalized sampling in Section II-B can be written in matrix form [22]. Similar to (10), we can assume any graph signal  $\mathbf{x}$  is modeled by a known generator matrix  $\mathbf{A} \in \mathbb{R}^{N \times K}$  ( $K \leq N$ ) and expansion coefficients  $\mathbf{d} \in \mathbb{R}^K$  as follows:

$$\mathbf{x} := \mathbf{A}\mathbf{d}. \quad (18)$$

The graph sampling operator is a matrix  $\mathbf{S} \in \mathbb{R}^{N \times M}$  ( $M \leq N$ ) which, without loss of generality, is assumed to have linearly independent columns that span a sampling space,  $\mathcal{S} \subset \mathbb{R}^N$ . The sampled signal is then given by

$$\mathbf{c} := \mathbf{S}^\top \mathbf{x} \in \mathbb{R}^M. \quad (19)$$

Since  $\mathbf{A}$  is known, signal recovery may be given by using (14):

$$\tilde{\mathbf{x}} = \mathbf{A}\mathbf{H}\mathbf{c} = \mathbf{A}(\mathbf{S}^\top \mathbf{A})^\dagger \mathbf{S}^\top \mathbf{x}, \quad (20)$$

where the correction transform is given by  $\mathbf{H} = (\mathbf{S}^\top \mathbf{A})^\dagger$ . When the DS condition holds,  $(\mathbf{S}^\top \mathbf{A})^\dagger = (\mathbf{S}^\top \mathbf{A})^{-1}$ , and perfect recovery is obtained. In some cases, it may be better to select  $\mathbf{W} \neq \mathbf{A}$ , e.g., for more efficient implementation, so that the leftmost  $\mathbf{A}$  in (20) would be replaced with  $\mathbf{W}$  (as in Fig. 1(b)). Such predefined solutions have been studied in [7], [8], [22]. This is equivalent to the generalized sampling in Hilbert space described in Section II-B.

Major challenges in graph signal sampling are selection and optimization of the generation and sampling matrices  $\mathbf{A}$  and  $\mathbf{S}$ , as well as efficient implementation of the pseudoinverse above. In some cases, analogous to the SI setting in standard sampling, this inverse can be implemented by filtering in the graph Fourier domain, as we show in the next section. Next, we describe some typical graph signal models (i.e., specific  $\mathbf{A}$ 's) as well as two sampling approaches (i.e., choices of  $\mathbf{S}$ ).

### B. Graph signal models

While the signal generation and recovery models of (18) and (20) are valid for any arbitrary signal subspace represented by  $\mathbf{A}$ , here we focus on choices of  $\mathbf{A}$  that are related to the specific graph  $\mathcal{G}$  on which we wish to process data. For example, the *bandlimited signal model* has been widely studied. This model corresponds to  $\mathbf{A} = \mathbf{U}_{\mathcal{V}\mathcal{B}}$  where  $\mathcal{B} := \{1, \dots, B\}$ . A bandlimited signal is thus written by

$$\mathbf{x}_{\text{BL}} = \sum_{i=1}^B d_i \mathbf{u}_i = \mathbf{U}_{\mathcal{V}\mathcal{B}} \mathbf{d}, \quad (21)$$

$\omega := \lambda_B$  is called the *bandwidth* or *cut-off frequency* of the graph signal. The signal subspace of  $\omega$ -bandlimited graph signals on  $\mathcal{G}$  is often called the *Paley-Wiener space*  $PW_\omega(\mathcal{G})$  [10], [11].

A more general frequency domain, but non-bandlimited, model could be obtained as

$$\mathbf{x} := \sum_{i=1}^K d_i \sum_{j=1}^N \hat{a}_i(\lambda_j) \mathbf{u}_j = \mathbf{A}\mathbf{d}, \quad (22)$$

where  $\mathbf{d} \in \mathbb{R}^M$  and the  $i$ -th column of  $\mathbf{A}$  is  $\sum_{j=1}^N \hat{a}_i(\lambda_j) \mathbf{u}_j$ . In this case each of the  $\hat{a}_i(\lambda)$  imposes a certain spectral shape (e.g., exponential) and the parameter  $d_i$  controls how much weight is given to the  $i$ -th spectral shape.

Another signal model that parallels those studied in the SI setting is described in the box “Periodic graph spectrum subspace”. This approach leads to recovery methods based on filtering in graph frequency domain, similar to (15).

The choice of  $\mathbf{A}$  can also be based on vertex domain graph signal properties. Let  $\{\mathcal{T}_i\}$  ( $i = 1, \dots, K$ ) be a partition of  $\mathcal{V}$ , where each node in  $\mathcal{T}_i$  is locally connected within the cluster. A piecewise constant graph signal is then given by

$$\mathbf{x}_{\text{PC}} = \sum_{i=1}^K d_i \mathbf{1}_{\mathcal{T}_i} = [\mathbf{1}_{\mathcal{T}_1}, \dots, \mathbf{1}_{\mathcal{T}_K}] \mathbf{d} \quad (23)$$

where  $[\mathbf{1}_{\mathcal{T}_i}]_n = 1$  when the node  $n$  is in  $\mathcal{T}_i$ ; 0 otherwise [23]. In this case,  $\mathbf{A} = [\mathbf{1}_{\mathcal{T}_1}, \dots, \mathbf{1}_{\mathcal{T}_K}]$ . Piecewise smooth graph signals can be similarly defined.

### Periodic graph spectrum subspace

To connect signal generation models of graph signals to those of SI signals, the *periodic graph spectrum (PGS)* subspace has been proposed in [7], [8]:

**Definition 1** (PGS Subspace). *An  $M$ -dimensional PGS subspace, where  $M \leq N$ , of a given graph  $\mathcal{G}$  is a space of graph signals that can be expressed as a GFT spectrum filtered by a given generator:*

$$\mathcal{X}_{\text{PGS}} = \left\{ x[n] \left| x[n] = \sum_{i=0}^{N-1} d(\lambda_i \bmod M) \hat{a}(\lambda_i) u_i[n] \right. \right\}, \quad (24)$$

where  $\hat{a}(\lambda_i)$  is the graph frequency domain response of the generator and  $d(\lambda_i)$  is an expansion coefficient.

A signal in a PGS subspace can be represented in matrix form as:

$$\mathbf{x}_{\text{PGS}} := \mathbf{A}_{\text{PGS}} \mathbf{d} = \mathbf{U} \hat{\mathbf{a}}(\mathbf{\Lambda}) \mathbf{D}_{\text{samp}}^{\top} \mathbf{d} \quad (25)$$

where  $\mathbf{d} := [d(\lambda_1), \dots, d(\lambda_{M-1})]^{\top}$  and  $\mathbf{D}_{\text{samp}}$  is given in (29). Definition 1 assumes the graph spectrum is periodic; importantly,  $\mathbf{x}$  is not necessarily bandlimited.

The PGS subspace is related to the signal subspace of *continuous-time* SI signals in (12). Suppose that  $T$  in (12) is a positive integer, i.e., the spectrum  $D(e^{j\omega T})$  is repeated  $T$  times within  $\omega \in [0, 2\pi]$ , and  $A(\omega)$  in (12) has support  $\omega \in [0, 2\pi]$ . In this case, a sequence  $X[i] = D(e^{j\omega T})A(\omega)|_{\omega=2\pi i/N}$  ( $i = 0, \dots, N-1$ ) corresponds to the DFT spectrum of length  $N$ . Therefore, this  $X[i]$  can be regarded as a graph signal spectrum in a PGS subspace if the GFT is identical to the DFT (by relaxing to a complex  $\mathbf{U}$ ), e.g., the graph  $\mathcal{G}$  is a cycle graph, i.e., a periodic graph consists of a ring. This relationship is illustrated in Fig. 2.

The correction filter  $\mathbf{H} = (\mathbf{S}^{\top} \mathbf{A})^{\dagger}$  for signals in a PGS subspace mimics the frequency response of (15). Suppose that graph frequency domain sampling in Definition 3 is used. The DS condition in this case implies  $\tilde{R}_{ga}(\lambda_i) \neq 0$  for all  $i = 1, \dots, M$ , where  $\tilde{R}_{ga}(\lambda_i) := \sum_{\ell} \hat{g}(\lambda_{i+M\ell}) \hat{a}(\lambda_{i+M\ell})$ . If  $\mathbf{x} \in \mathcal{X}_{\text{PGS}}$  and the DS condition holds, then the correction transform  $\mathbf{H}$  is equivalent to filtering in the graph frequency domain with correction filter [7]

$$\hat{h}(\lambda_i) = \frac{1}{\tilde{R}_{ga}(\lambda_i)}, \quad (26)$$

which clearly parallels the SI expression (15).

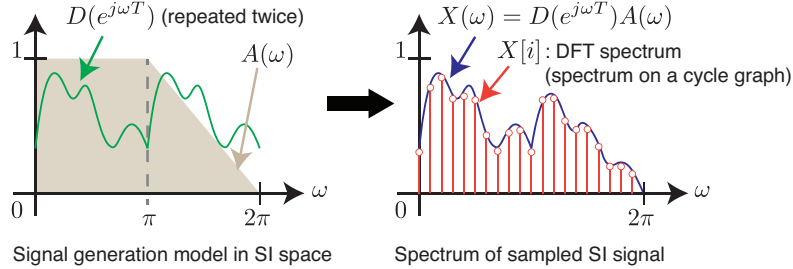


Fig. 2: Relationship between PGS and SI signals for  $T = 2$ .

### C. Sampling methods

Similar to time and frequency domain sampling for conventional signals, graph signal sampling can be defined in both the spectral and vertex domains. For time domain signals, there is a simple relationship between sampling in both domains, as can be seen from (11) and (12). In contrast, for general graphs direct node-wise sampling in the vertex domain (i.e., selecting a subset of nodes) does not correspond to a spectrum folding operation in the graph frequency domain, and vice versa. Thus, we discuss vertex and frequency domain graph sampling separately.

1) *Vertex Domain Sampling*: Vertex domain sampling is an analog of time domain sampling. Samples are selected on a predetermined *sampling set*,  $\mathcal{T} \in \mathcal{V}$ , containing which  $|\mathcal{T}| = M$  nodes. Sampling set selection is described later in Section IV. For a given  $\mathcal{T}$  we define sampling as follows:

**Definition 2** (Vertex domain sampling [9], [11]). *Let  $\mathbf{x} \in \mathbb{R}^N$  be a graph signal and  $\mathbf{G} \in \mathbb{R}^{N \times N}$  be an arbitrary graph filter in (2). Suppose that the sampling set  $\mathcal{T}$  is given a priori. The sampled graph signal  $\mathbf{c} \in \mathbb{R}^M$  is defined by:*

$$\mathbf{c} = \mathbf{I}_{\mathcal{T}\mathcal{V}} \mathbf{G} \mathbf{x}, \quad (27)$$

where  $\mathbf{I}$  is the  $N \times N$  identity matrix.

The sampling matrix is therefore given by  $\mathbf{S}^\top = \mathbf{I}_{TV}\mathbf{G}$ . Many methods in the literature consider direct sampling, where  $\mathbf{G} = \mathbf{I}$ . An alternative is aggregation sampling [12], [24] where  $\mathbf{G}$  corresponds to a filtering operation prior to sampling.

2) *Graph Frequency Domain Sampling*: Sampling in the graph frequency domain [14] parallels Fourier domain sampling in (6): The graph Fourier transformed input  $\hat{\mathbf{x}}$  is first multiplied by a graph spectral filter  $\hat{g}(\Lambda)$ ; the product is subsequently folded with period  $M$ , resulting in aliasing for non-bandlimited signals, which can be utilized for the design of graph wavelets/filter banks [13], [25]. Graph frequency domain sampling is defined as follows:

**Definition 3** (Graph frequency domain sampling). *Let  $\hat{\mathbf{x}} \in \mathbb{R}^N$  be the original signal in the graph frequency domain, i.e.,  $\hat{\mathbf{x}} = \mathbf{U}^\top \mathbf{x}$ , and let  $\hat{g}(\Lambda)$  be an arbitrary sampling filter expressed in the graph frequency domain. For a sampling ratio  $M \in \mathbb{Z}$  where  $M$  is assumed to be a divisor of  $N$  for simplicity, the sampled graph signal in the graph frequency domain is given by*

$$\mathbf{c} = \mathbf{D}_{\text{samp}} \hat{g}(\Lambda) \hat{\mathbf{x}}, \quad (28)$$

where

$$\mathbf{D}_{\text{samp}} = \begin{bmatrix} \mathbf{I}_M & \mathbf{I}_M & \dots \end{bmatrix} \quad (29)$$

is the spectrum folding matrix.

The sampling matrix  $\mathbf{S}^\top$  in the graph frequency domain is thus given by

$$\mathbf{S}^\top = \mathbf{D}_{\text{samp}} \hat{g}(\Lambda) \mathbf{U}^\top. \quad (30)$$

While this definition is clearly an analog of Frequency domain sampling in (6), in general it cannot be written as an operator of the form of  $\mathbf{I}_{TV}\mathbf{G}$ , i.e., graph filtering, as defined in Section II-A, and vertex domain sampling, except for some specific cases, such as cycle or bipartite graphs [7], [14], [26]. See box “Illustrative example of sampling procedures” for a comparison between graph signal sampling and conventional discrete-time signal sampling.

#### Illustrative example of sampling procedures

In Fig. 3 (left) standard discrete-time sampling is shown in both time and frequency domains. Point-wise sampling in the time domain corresponds to folding of the DFT spectrum [1], [27]. Note that both sampling methods yield the same output after the inverse DFT of the frequency sampled signal. Fig. 3 (right) illustrates graph signal sampling in vertex and graph frequency domains (Definitions 2 and 3), which do not yield the same output, unlike their conventional signal counterparts of Fig. 3 (left).

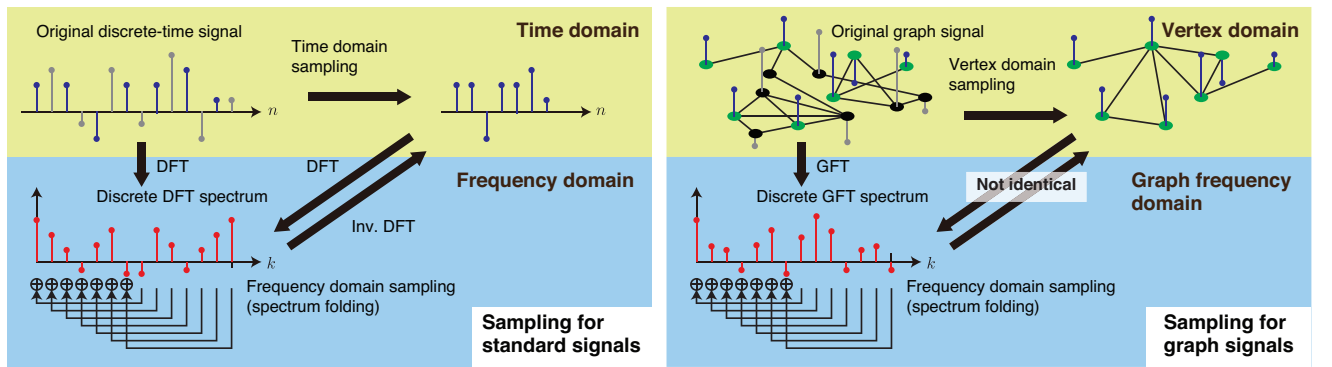


Fig. 3: Sampling procedures for standard and graph signals.

#### D. Remarks on correction and reconstruction transforms

In the SI setting, signal recovery can be implemented in the time domain as (9) with counterparts in the Fourier domain as in (15). However, this is not the case for vertex domain sampling: While the sampling matrix  $\mathbf{S}$  in Definition 2 is designed to parallel sampling in the time domain, the correction matrix  $\mathbf{H} = (\mathbf{S}^\top \mathbf{A})^\dagger$  does not have a diagonal graph frequency response

in general. Refer to the box “Bandlimited signal recovery with vertex domain sampling” for an example with bandlimited signals. One exception is the PGS setting (see the box “Periodic graph spectrum subspace”) where  $\mathbf{H}$  can be implemented in the graph Fourier domain as in (26).

In this section, for simplicity we have considered the case where measurement, sampling, and recovery are noise-free. In the presence of noise, the reconstruction of (20) may be replaced by noise-robust methods. See the box “Different reconstruction operators” for an example. Note that the recovery procedures for the noisy cases have been well studied in the context of (generalized) sampling theory for standard signals [1] as well as compressed sensing [28]. Robustness against noisy measurements is also a major motivation to optimize sampling set selection of graphs (see next section).

#### Bandlimited signal recovery with vertex domain sampling

Assume we have a bandlimited signal  $\mathbf{x}_{\text{BL}}$  as defined in (21) and we use the direct node-wise sampling, i.e.,  $\mathbf{G} = \mathbf{I}$ . This is a well-studied setting for graph sampling theory. The DS condition in this case is often called the *uniqueness set* condition [10], [11] and requires a full-rank  $\mathbf{I}_{\mathcal{T}\mathcal{V}}\mathbf{U}_{\mathcal{V}\mathcal{B}} = \mathbf{U}_{\mathcal{T}\mathcal{B}} \in \mathbb{R}^{M \times M}$  [9], [11] (we assume  $M = B$ ). In this case, we have  $\mathbf{A} = \mathbf{U}_{\mathcal{V}\mathcal{B}}$  and (20) is reduced to

$$\tilde{\mathbf{x}} = \mathbf{U}_{\mathcal{V}\mathcal{B}}(\mathbf{U}_{\mathcal{T}\mathcal{B}})^\dagger \mathbf{c}, \quad (31)$$

note that we assume  $M = |\mathcal{T}| = |\mathcal{B}|$ . In other words, the correction transform is given by  $\mathbf{H} = (\mathbf{U}_{\mathcal{T}\mathcal{B}})^\dagger$ . Note that  $\mathbf{H}$  cannot be written as a graph spectral filter having a diagonal frequency response. Even if the sampling filter  $\mathbf{G}$  is applied before node-wise sampling such as aggregation sampling [12], [24], the perfect or LS recovery is obtained by replacing  $(\mathbf{U}_{\mathcal{T}\mathcal{B}})^\dagger$  in the above equation with  $(\mathbf{G}_{\mathcal{T}\mathcal{V}}\mathbf{U}_{\mathcal{V}\mathcal{B}})^\dagger$  while  $\mathbf{A} = \mathbf{U}_{\mathcal{V}\mathcal{B}}$  does not change. An approximate recovery of bandlimited graph signals is possible with an alternative approach, e.g., an iterative algorithm using polynomial filters and projection onto convex sets [29].

#### Different reconstruction operators

The reconstruction in (20) allows for perfect signal recovery under the DS condition, when the signal lies in a given subspace. However, we may not always have such a strong prior. For example, we may only know that our signal is smooth in some sense. A popular approach in this case is to consider the following recovery approach [1], [28]:

$$\tilde{\mathbf{x}} = \arg \min_{\mathbf{S}^\top \mathbf{x} = \mathbf{c}} \|\mathbf{V}\mathbf{x}\|_p, \quad (32)$$

where  $\mathbf{V}$  is a matrix that measures smoothness (examples are introduced in Section III-B). If there is noise, we can relax the goal of achieving a consistent solution, i.e., such that  $\mathbf{S}^\top \mathbf{x} = \mathbf{S}^\top \tilde{\mathbf{x}}$ , and instead solve the following problem:

$$\tilde{\mathbf{x}} = \arg \min_{\mathbf{x} \in \mathbb{R}^N} \|\mathbf{S}^\top \mathbf{x} - \mathbf{c}\|_2^2 + \gamma \|\mathbf{V}\mathbf{x}\|_p \quad (33)$$

where  $\gamma > 0$  is a regularization parameter. Fast and efficient interpolation algorithms have also been studied in [30]–[33] based on generalizations of standard signal processing techniques to the graph setting.

#### E. Signal recovery experiments

To illustrate signal recovery for both bandlimited and full-band settings, we consider the random sensor graph example of Fig. 4, with  $N = 64$  and  $M = 10$ . The first scenario is the well-known bandlimited setting, where the signal is bandlimited as in (21) with  $B = 10$  and the sampling filter is the identity matrix, i.e.,  $\mathbf{G} = \mathbf{I}$ . In the second scenario, we use the non-bandlimited generator in the graph frequency domain with the PGS model [7], [8] (see the box “Periodic graph spectrum subspace”). The generator function is  $\hat{a}(\lambda_i) = 1 - 2\lambda_i/\lambda_{\max}$  and each element in  $\mathbf{d} \in \mathbb{R}^M$  is drawn from  $\mathcal{N}(1, 1)$ . The sampling filter is also non-bandlimited where  $\hat{g}(\lambda_i) = \exp(-\lambda_i/2)$ .

As shown in Fig. 4 (top), both vertex and frequency sampling methods can recover the bandlimited graph signal. Note that  $\mathbf{c}$  is identical to  $\mathbf{d}$  for graph frequency domain sampling. In contrast, Fig. 4 (bottom) shows that the original signal oscillates in the vertex domain due to its full-band generator function. Also,  $\mathbf{c}$  of graph frequency domain sampling does not match the original spectrum due to aliasing and the sampling filter. But, even in that case, the original signal is perfectly recovered when the signal subspace is given.



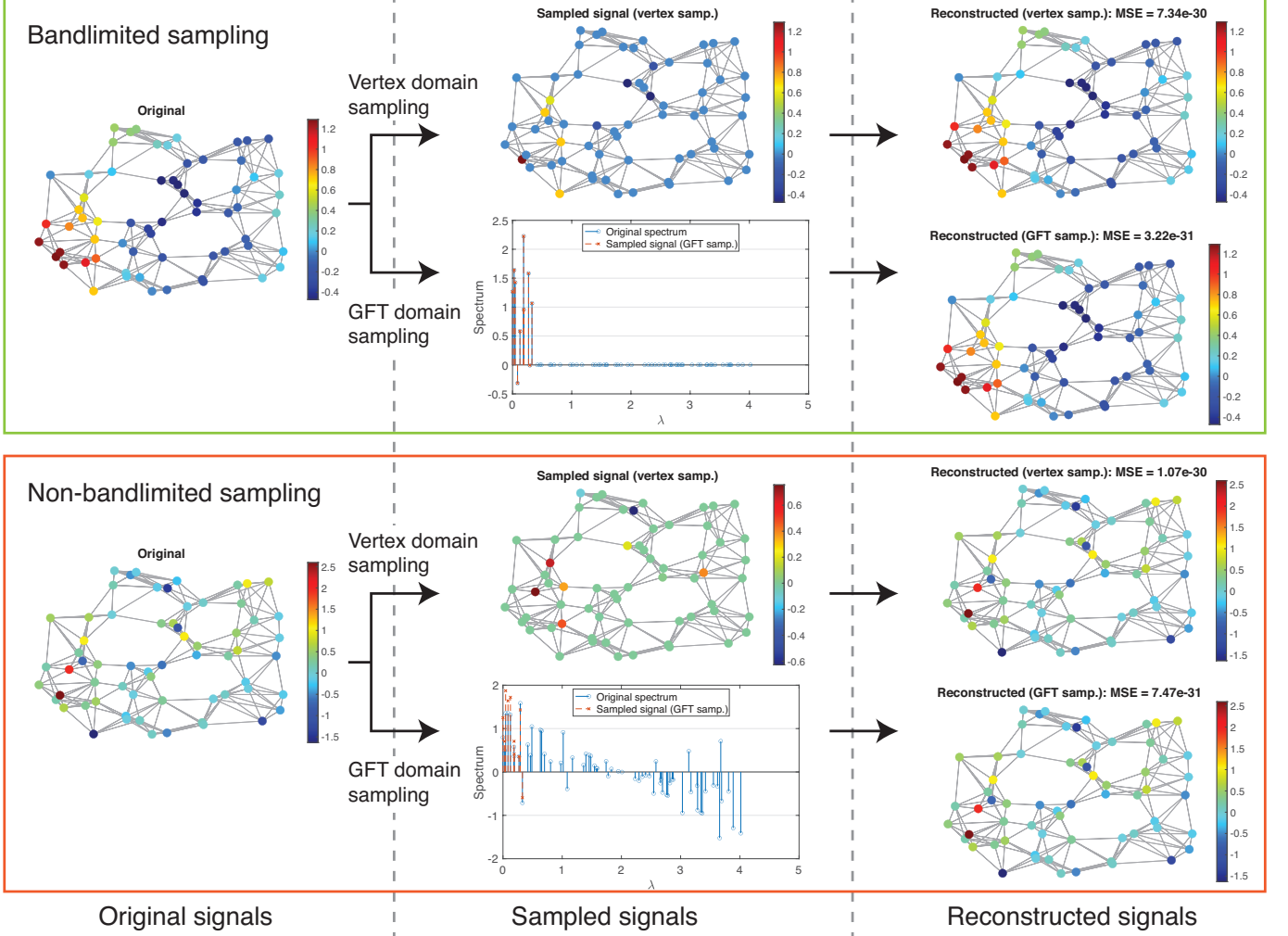


Fig. 4: Sampling examples for signals on a random sensor graph with  $N = 64$ . The sample  $\mathbf{c}$  has length  $M = 10$ . Top: Bandlimited sampling where the signal is bandlimited with  $B = 10$  and the sampling filter is the identity matrix. Bottom: Non-bandlimited sampling, where the generator function is generated by the PGS model [7], [8] with the generator function  $\hat{a}(\lambda_i) = 1 - 2\lambda_i/\lambda_{\max}$  and the sampling function is  $\hat{g}(\lambda_i) = \exp(-\lambda_i/2)$  (see also the box “Periodic graph spectrum subspace”). Even in this case, the original signal is perfectly recovered from  $\mathbf{c}$  by using both of vertex and graph frequency domain sampling without changing the framework.

#### IV. SAMPLING SET SELECTION AND EFFICIENT COMPUTATION METHODS

In this section, efficient sampling set selection methods for vertex domain sampling are examined. The recovery method in (20) can be possible only if the signal subspace, e.g., cut-off frequency, is known perfectly *a priori*. However, in practice the cut-off frequency is often unknown (and thus can at best be estimated), or the signal is smooth but not strictly bandlimited in the first place. Further, observed samples may be corrupted by additive noise. Thus, practical sampling set selection algorithms often aim at maximizing robustness to noise or imperfect knowledge of sampled signal characteristics.

Along with signal reconstruction quality, computational complexity is another key concern when designing sampling algorithms since signals often reside in very large graphs. Often, one would like to avoid computing the eigen-decomposition of the chosen graph variation operator, such as the graph Laplacian matrix, which requires large computational cost ( $\mathcal{O}(N^3)$  in the general case). We next provide an overview of fast and efficient sampling set selection methods.

### A. Sampling set selection: Deterministic and random approaches

A list of representative sampling methods is given in Table I. One of the first considerations when deciding on a sampling scheme is whether a deterministic or random approach should be chosen. Deterministic approaches [9], [11], [12], [16], [29], [34]–[37] choose a fixed node subset to optimize a pre-determined cost function. Since sampling set selection is in general combinatorial and NP-hard, many deterministic selection methods are greedy, adding one locally optimal node at a time until the sampling budget is exhausted. Advantages of deterministic sampling set selection methods include: i) “Importance” of individual nodes are computed and totally ordered for greedy selection; if the sampling budget changes, one can add or remove nodes easily without re-running the entire selection algorithm, and ii) the selected node subset remains fixed as long as the graph structure is the same.

In contrast, random methods [38], [39] select nodes randomly according to a pre-determined probability distribution. Typically, the distribution is designed so that more “important” nodes are selected with higher probabilities. One key merit of a random method is low computation cost. Once the probability distribution is determined, the selection itself can be realized quickly in a distributed manner. In practice, random sampling methods may perform well on average, but often require more samples than deterministic methods to achieve the same reconstruction quality even if the signal is bandlimited [38]. One may also combine deterministic and random selection methods to find a sampling set.

### B. Deterministic Sampling Set Selection

Two main types of deterministic sampling set selection methods have been proposed in the literature. First, vertex-based methods have been studied extensively in machine learning and sensor network communities as a sensor placement problem (see further discussion on applications in Section V). Second, spectrum-based methods—selection schemes grounded in graph frequency assumptions—represent a relatively new approach and have been studied in the context of graph sampling theory. We focus on the latter approach due to space limitation. See [13] for a summary of existing vertex-based methods.

**Exact bandlimited case:** For simplicity suppose we directly observe the samples, i.e.,  $\mathbf{G} = \mathbf{I}$ , and choose a bandlimited signal model in (21). To optimize the sampling set we can define an objective function to quantify reconstruction error in the presence of noise. The sampled signal  $\mathbf{y} \in \mathbb{R}^M$  is then:

$$\mathbf{y} = \mathbf{c} + \mathbf{n}, \quad (34)$$

where  $\mathbf{n}$  is an i.i.d. additive noise introduced during the measurement or sampling process. Using the LS recovery (17), the reconstructed signal  $\tilde{\mathbf{x}}$  is then given by

$$\tilde{\mathbf{x}} = \mathbf{U}_{\mathcal{V}\mathcal{B}} \mathbf{U}_{\mathcal{T}\mathcal{B}}^\dagger \mathbf{y} = \mathbf{U}_{\mathcal{V}\mathcal{B}} \mathbf{U}_{\mathcal{T}\mathcal{B}}^\dagger \mathbf{c} + \mathbf{U}_{\mathcal{V}\mathcal{B}} \mathbf{U}_{\mathcal{T}\mathcal{B}}^\dagger \mathbf{n}. \quad (35)$$

LS reconstruction error thus becomes  $\mathbf{e} := \tilde{\mathbf{x}} - \mathbf{x} = \mathbf{U}_{\mathcal{V}\mathcal{B}} \mathbf{U}_{\mathcal{T}\mathcal{B}}^\dagger \mathbf{n}$ . Many deterministic methods choose an optimization objective based on the error covariance matrix:

$$\mathbf{E} := \mathbb{E}[\mathbf{e}\mathbf{e}^\top] = \mathbf{U}_{\mathcal{V}\mathcal{B}} (\mathbf{U}_{\mathcal{T}\mathcal{B}}^\top \mathbf{U}_{\mathcal{T}\mathcal{B}})^{-1} \mathbf{U}_{\mathcal{V}\mathcal{B}}^\top. \quad (36)$$

Given (36), one can choose different optimization criteria based on optimal design of experiments [40]. For example, the *A-optimality* criterion minimizes the average errors by seeking  $\mathcal{T}$  which minimizes the trace of the matrix inverse [15]:

$$\min_{\mathcal{T} \mid |\mathcal{T}|=M} \text{Tr}((\mathbf{U}_{\mathcal{T}\mathcal{B}}^\top \mathbf{U}_{\mathcal{T}\mathcal{B}})^{-1}), \quad (37)$$

while *E-optimality* minimizes the worst-case errors by maximizing the smallest eigenvalue of the information matrix  $\mathbf{U}_{\mathcal{T}\mathcal{B}}^\top \mathbf{U}_{\mathcal{T}\mathcal{B}}$  [9]:

$$\max_{\mathcal{T} \mid |\mathcal{T}|=M} \lambda_{\min}(\mathbf{U}_{\mathcal{T}\mathcal{B}}^\top \mathbf{U}_{\mathcal{T}\mathcal{B}}) \quad (38)$$

In either case, sampling set selection based on error covariance matrix (36) requires (partial) singular value decomposition (SVD) of an  $M \times M$  matrix, even when the GFT matrix  $\mathbf{U}$  is given *a priori*. This results in a large computation cost. To alleviate this burden, greedy sampling without performing SVD has been recently proposed. This category includes methods using spectral proxies which approximately maximize cut-off frequency [11], two-step algorithms which first calculate a

TABLE I: Comparison of Graph-based Sampling Set Selection Methods.

Methods	Deterministic/ random	Kernel	Localization in vertex domain	Localization in graph freq. domain
Maximizing cutoff freq. [11]	Deterministic	$\lambda^k$ ( $k \in \mathbb{Z}_+$ )		✓
Error covariance [9], [15]	Deterministic	Ideal		✓
Vertex screening [41]	Deterministic	Ideal	✓	✓
Localized operator [13]	Deterministic	Arbitrary	✓	✓
Neumann Series [42]	Deterministic	Ideal	✓*	✓
Gershgorin disc alignment [16]	Deterministic	$\lambda$	✓	
Cumulative coherence [38]	Random	Ideal	✓*	✓
Global/local uncertainty [39]	Random	Arbitrary	✓	✓

\* Localized in the vertex domain only if the ideal kernel is approximated by a polynomial

permissible set and then select a node within the set [41], a graph filter submatrix that avoids SVD by utilizing a fast GFT and block matrix inversion [42], and a polynomial filtering-based approach that maximizes a vertex domain support of graph spectral filters [13].

**Smooth signals:** Instead of a strict bandlimited assumption, one can assume the target signal  $\mathbf{x}$  is smooth with respect to the underlying graph, where smoothness is measured via operator  $\mathbf{V}$ . One can thus reconstruct via a regularization-based optimization in (33); in [16],  $\mathbf{V} = \mathbf{L}^{1/2}$  and the reconstruction becomes:

$$\min_{\mathbf{x}} \|\mathbf{S}^\top \mathbf{x} - \mathbf{y}\|_2^2 + \gamma \mathbf{x}^\top \mathbf{L} \mathbf{x}. \quad (39)$$

Problem (39) has a closed form solution  $\mathbf{x}^*$ :

$$\mathbf{x}^* = (\mathbf{S}\mathbf{S}^\top + \gamma \mathbf{L})^{-1} \mathbf{S} \mathbf{y}. \quad (40)$$

Authors in [16] then choose the sampling matrix  $\mathbf{S}^\top$  to maximize the smallest eigenvalue  $\lambda_{\min}$  of the coefficient matrix  $\mathbf{S}\mathbf{S}^\top + \gamma \mathbf{L}$  in (40)—corresponding to the E-optimality criterion. This is done without eigen-decomposition via a novel usage of the well-known Gershgorin circle theorem.

**Relationship between various methods based on localized operator:** Vertex and spectrum-based methods have been proposed separately in different research fields. Interestingly, many of them can be described in a unified manner by utilizing a graph localization operator [13]. A graph localization operator is a vertex domain expression of a spectral filter kernel  $\hat{g}(\lambda)$  centered at the node  $i$  [39]:

$$\psi_{g,i}[n] := \sqrt{N} \sum_{k=1}^N \hat{g}(\lambda_k) u_k[i] u_k[n], \quad (41)$$

which can be viewed as the “impulse response” of a graph filter by rewriting (41) in vector form as

$$\boldsymbol{\psi}_{g,i} = \mathbf{U} \hat{g}(\boldsymbol{\Lambda}) \mathbf{U}^\top \boldsymbol{\delta}_i, \quad (42)$$

where  $\boldsymbol{\delta}_i$  is an indicator vector for the  $i$ th node, i.e., unit impulse. In [13], it has been shown that many proposed cost functions can be interpreted as having the form of (42) for different kernels.

### C. Random Sampling Set Selection

Random selection methods can be classified into two categories. First, graph-independent approaches select nodes randomly without taking into account the underlying graph [9], [24], [38], which results in very low computational cost. However, theoretical results based on studies on compressed sensing [24], [38] have shown that the number of required nodes for recovery of bandlimited graph signals tends to be larger than for graph-dependent selections [38].

Second, graph-dependent random selection methods [38], [39] assume that node importance varies according to the underlying graph, i.e., important nodes are connected to many other nodes with large edge weights. In these approaches, a sampling probability distribution  $\mathbf{p} \in \mathbb{R}^N$ , where  $p[i] \geq 0$  for all  $i$  ( $i = 0, \dots, N-1$ ) and  $\sum_i p[i] = 1$ , is first obtained prior to running a random selection algorithm. Once  $\mathbf{p}$  is obtained, the sampling set is randomly chosen based on  $\mathbf{p}$ .

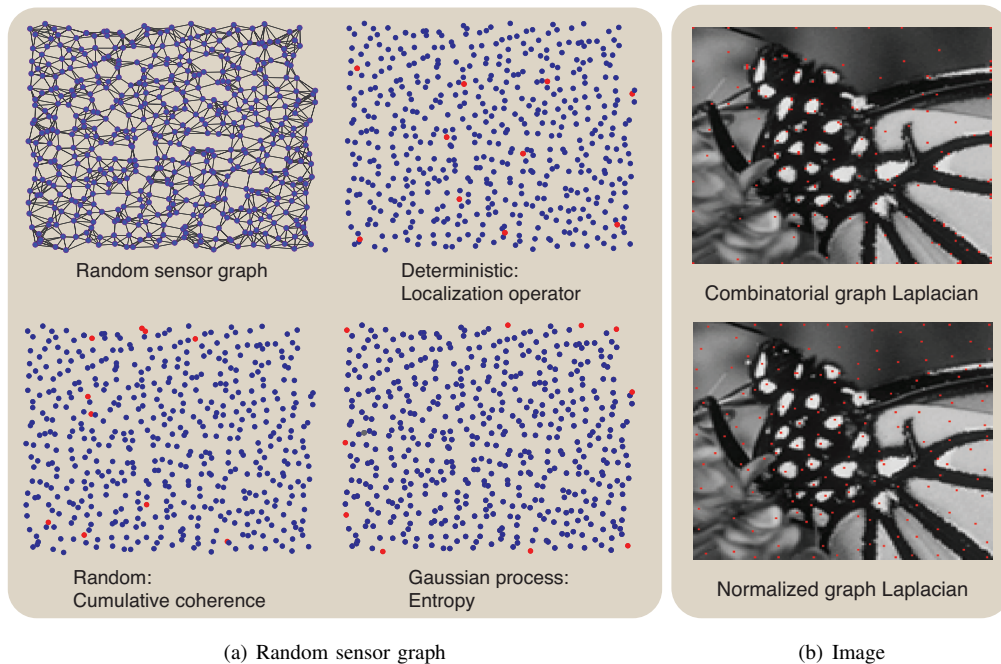


Fig. 5: Comparison of sampling sets. (a) Sampling sets for a random sensor graph with  $N = 500$ , and 10 nodes from that graph are selected. From left to right: The original graph, sampling set by a deterministic approach [13], sampling set of one realization by a random approach [38], sampling set by a Gaussian process-based method [43]. (b) Sampling sets for image pixels. Each pixel is a node, and edge weights are chosen based on [44]. The sampling set selection method based on maximizing cut-off frequency [11] is used. Top and bottom: Sampling set selected using the combinatorial and normalized graph Laplacians, respectively.

As an example, in the graph coherence-based random selection method for  $\omega$ -bandlimited graph signals of [38], the sampling distribution is given as follows:

$$p[i] := \|\mathbf{U}_{\mathcal{V}_B}^\top \boldsymbol{\delta}_i\|_2^2 / B \quad (43)$$

where the numerator is the same as  $\|\boldsymbol{\psi}_{g,i}\|_2^2$  in (42) with  $\hat{g}(\lambda)$  is the bandlimiting filter. To avoid eigen-decomposition, a polynomial approximation for the filter can be applied and the calculation cost can be further reduced by filtering random signals instead of  $\boldsymbol{\delta}_i$ ,  $i = 0, \dots, N - 1$ . A similar approach has been using an arbitrary filter kernel  $\hat{g}(\lambda)$  has also been proposed [39].

#### D. Sampling set selection examples

As a first example, Fig. 5(a) shows sampling sets of size 10 for a random sensor graph with  $N = 500$ . These methods are compared: i) a deterministic method based on localized operator [13], ii) a graph-dependent random selection method using cumulative coherence [38], and iii) a traditional entropy-based sensor selection method [43]. Random methods may select nodes close to each other, as can be seen in this realization, while the entropy-based method tends to favor low degree nodes leading to samples close to the boundary [13]. Instead, the deterministic approach selects nodes that are more uniformly distributed in space.

In the second example, Fig. 5(b), we use graph signal sampling to select pixels in an image. Each graph node correspond to a pixel and edge weights are selected using [44], sampling set selection is based on maximizing cut-off frequency [11]. We used two variation operators, the combinatorial and symmetric normalized graph Laplacians, leading to very different sampling sets. When using the combinatorial Laplacian selected tend to be closer to image contours or the image boundary. In contrast, pixels selected using the normalized Laplacian are more uniformly distributed within the image. See also the box “To normalize, or not to normalize” for a comparison of variation operators.

### To normalize, or not to normalize

Different graph variation operators lead to different sampling sets, as shown in Fig. 5(b). This difference in behavior is due to normalization. As an example, consider a three-cluster graph with  $N = 27$  [45], and compare combinatorial graph Laplacian and its symmetric normalized version, with sampling set selection based on maximizing cut-off frequency [11], as seen in Fig. 6.

In Fig. 6 color represents node selection order (first chosen nodes are blue, while last chosen ones are red). Observe that for the combinatorial Laplacian (Fig. 6 right), most nodes in cluster A are selected in the last stage, while for the normalized graph Laplacian (Fig. 6 left), nodes in cluster A are selected at all stages. This is due to the localization of the GFT bases: Eigenvectors of the combinatorial graph Laplacian are localized in the vertex domain compared to the normalized one. This is illustrated by the spectral representations in Fig. 6, using the visualization technique in [45]; eigenvectors corresponding to low (high) graph frequencies are located at the bottom (top) of the figure. In this figure, the sampling orders are also illustrated as red circles (early selected nodes are located at the bottom). Clearly, high frequency eigenvectors of the combinatorial graph Laplacian are highly localized in cluster A, so that the method in [11] selects nodes in cluster A more likely in its last stage. In contrast, for the normalized version, the eigenvectors are less localized, so that selected nodes are more balanced among clusters.

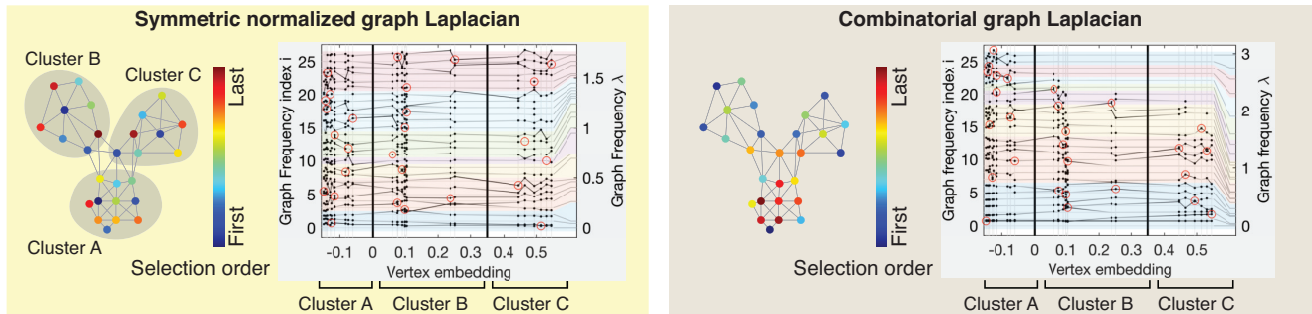


Fig. 6: Selection orders for different variation operators and oscillations of eigenvectors.

### E. Computational complexity

Computing a sampling set selection can be divided into two phases: i) *Preparation*, which includes computing required prior information, e.g., the eigen-decomposition, and ii) *Selection*, the main routine that selects nodes for sampling. Computational complexities of different methods are summarized next.

1) *Deterministic Selection*: Deterministic selection methods, studied in the context of graph sampling theory, basically need to calculate eigen-pair of (a part of) the variation operator in the selection phase. Their computation costs mostly depend on the number of edges in the graph and the assumed bandwidth. A recent trend is to investigate eigen-decomposition-free sampling set selection algorithms [13], [16], [42]. These recent methods approximate a graph spectral cost function with vertex-domain processing like polynomial approximation of the filter kernel. Table II shows that the computational complexities of these eigen-decomposition-free methods compare well with previous sampling methods [9], [11], [34] that require computation of multiple eigen-pairs.

2) *Random Selection*: Random selection methods typically entail a much smaller computation cost the selection phase than their deterministic counterparts. As discussed, given a sampling probability distribution  $\mathbf{p}$ , all sampled nodes can be chosen quickly and in parallel using  $\mathbf{p}$ . Hence, only the preparation phase needs to be considered. For graph-independent random selection,  $p[i] = 1/N$  for all  $i$ , and its computation cost is negligible. Many graph-dependent approaches require repeated calculations of  $\mathbf{U}\hat{g}(\boldsymbol{\Lambda})\mathbf{U}^\top\mathbf{v}$ , where  $\mathbf{v} \in \mathbb{R}^N$  is a random vector or  $\delta_i$ . While the naïve implementation still requires eigen-decomposition, the graph filter response  $\hat{g}(\lambda)$  is often approximated by a polynomial: The preparation phase requires iterative vertex-domain processing. Typically,  $\mathbf{p}$  is estimated after  $L$  (typically  $L = 2 \log(N)$  [38]) filterings of random vectors, which leads to  $\mathcal{O}(LP(|\mathcal{E}| + N))$  complexity [38].

## V. APPLICATIONS

Graph sampling has been used across a wide range of applications, such as wireless communications, data mining, or machine learning. We select a few interesting applications for in-depth discussion in this section.

TABLE II: Computational Complexities of GSP-Based Deterministic Sampling Set Selection

Method	Preparation	Selection
Maximizing cutoff freq. [11]	$O(k \mathcal{E} MT(k))$	$O(NM)$
Error covariance: E-optimal [9]	$O(( \mathcal{E} M + CM^3)T_B)$	$O(NM^4)$
Error covariance: A-optimal [9], [15]		$O(NM^4)$
Error covariance: T-optimal [15]		$O(NM)$
Error covariance: D-optimal [15]		$O(M^3)$
Localized operator [13]	$O(( \mathcal{E}  + N)P + J)$	$O(JM)$
Neumann series [42]	$O(N^2 \log^2 N)$	$O(NM^3)$
Gershgorin disc alignment [16]	$O(J \log_2(1/\eta))$	$O(MJ \log_2(1/\eta))$

Parameters.  $T(k)$ : Average number of iterations required for the convergence of a single eigen-pair where  $k$  is a trade-off factor between performance and complexity.  $T_B$ : The number of iterations of convergence for the first  $B$  eigen-pair.  $C$ : Constant,  $P$ : Approximation order of the Chebyshev polynomial approximation.  $J$ : The number of nonzero elements in the localization operator.  $\eta$ : numerical precision to terminate binary search in Gershgorin disc alignment.

### A. Sensor Placement

*Sensor placement* [43], [46]–[48] has long been studied in the wireless communication community. The basic problem is to choose a subset of locations from a discrete feasible set to place sensors, in order to monitor a physical phenomena such as temperature or radiation over a large geographical area of interest. Commonly, the field signal is assumed to be represented by a low-dimensional parameter vector with a measurement matrix  $\Phi$  generated by a Gaussian process [48]. Different criteria have been proposed to optimize the corresponding error covariance matrix, including A-optimality, E-optimality, D-optimality, and frame potential [46].

As one concrete example, one formulation is to maximize the smallest eigenvalue  $\lambda_{\min}$  of the inverse error covariance matrix (*information matrix*) via selection of a sensor subset  $\mathcal{T}$ , where  $|\mathcal{T}| = M$ :

$$\max_{\mathcal{T}, |\mathcal{T}|=M} \lambda_{\min}(\Phi_{\mathcal{T}\mathcal{V}}^\top \Phi_{\mathcal{T}\mathcal{V}}) \quad (44)$$

where  $\Phi_{\mathcal{T}\mathcal{V}}$  is a submatrix of  $\Phi$  with selected rows indicated by set  $\mathcal{T}$  and maximization leads to E-optimality [40] as mentioned in Section IV-B.

If the measurement matrix  $\Phi$  is the matrix  $\mathbf{V}_M$  containing the first  $M$  eigenvectors of a graph Laplacian matrix  $\mathbf{L}$ , then we can interpret (44) as a graph sampling problem under a  $M$ -bandlimited assumption. Sampling set selection methods described in Section IV can thus be used to solve (44). Specifically, recent fast graph sampling schemes [13], [49] have been used for sensor selection with improve execution speed and reconstruction quality compared to Gaussian process based methods.

### B. Sampling for Matrix Completion

*Matrix completion* [50] is the problem to fill or interpolate missing values in a partially observable matrix signal  $\mathbf{X} \in \mathbb{R}^{N_r \times N_c}$ , where  $N_r$  and  $N_c$  are often very large. One well-known example is the *Netflix challenge*<sup>1</sup>: in order to recommend movies to viewers, missing movie ratings in a large matrix, with viewers and movies as rows and columns respectively, are estimated based on a small subset of available viewer ratings. As an ill-posed problem, signal priors are required for regularization. One popular prior is the *low-rank prior* [51]: target matrix signal  $\mathbf{X}$  should be of low dimensionality, and thus low-rank. However,  $\text{rank}(\mathbf{X})$  is non-convex, and convexifying it to the nuclear norm  $\|\mathbf{X}\|_*$  (sum of singular values) still requires computing SVD per iteration in a proximal gradient method, which is expensive.

The underlying assumption of a low-rank prior is that the items along the rows and columns are similar. One can thus alternatively model these pairwise similarity relations using *two* graphs [52], [53]. Specifically, columns of  $\mathbf{X}$  are assumed to

<sup>1</sup>[https://en.wikipedia.org/wiki/Netflix\\_Prize](https://en.wikipedia.org/wiki/Netflix_Prize)

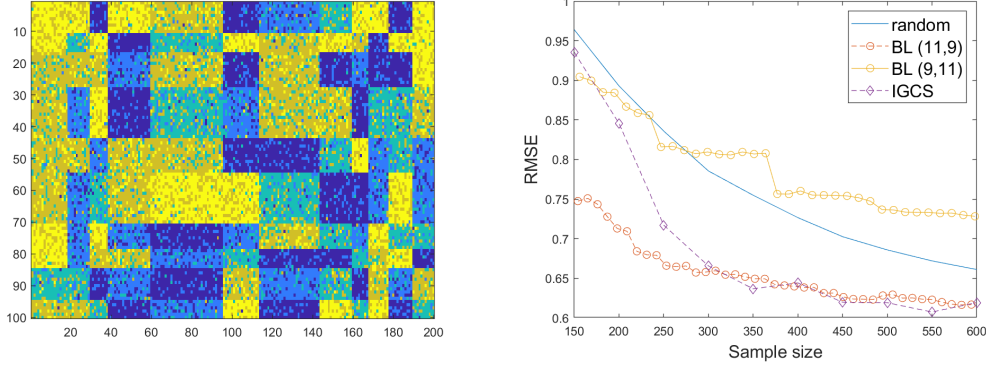


Fig. 7: (left) Example of a low-rank matrix and (right) Performance comparison of graph sampling algorithms (random, [53], [54]) for matrix completion in root mean squared error (RMSE).

be smooth with respect to an undirected weighted *row graph*  $\mathcal{G}_r = (\mathcal{V}_r, \mathcal{E}_r, \mathbf{W}_r)$  with vertices  $\mathcal{V}_r = \{1, \dots, m\}$  and edges  $\mathcal{E}_r \subseteq \mathcal{V}_r \times \mathcal{V}_r$ . Weight matrix  $\mathbf{W}_r$  specifies pairwise similarities among vertices in  $\mathcal{G}_r$ . The combinatorial graph Laplacian matrix of  $\mathcal{G}_r$  is  $\mathbf{L}_r = \mathbf{D}_r - \mathbf{W}_r$ , where the degree matrix  $\mathbf{D}_r$  is diagonal with entries  $[\mathbf{D}_r]_{ii} = \sum_j [\mathbf{W}_r]_{ij}$ . [53] then assume that all columns of matrix signal  $\mathbf{X}$  are bandlimited with respect to the graph frequencies defined using  $\mathbf{L}_r$ . Alternative to strict bandlimitedness, [52] assume that the columns of matrix signal  $\mathbf{X}$  are smooth with respect to  $\mathbf{L}_r$ , resulting a small  $\text{Tr}(\mathbf{X}^\top \mathbf{L}_r \mathbf{X})$ .

Similarly, one can define a *column graph*  $\mathcal{G}_c = (\mathcal{V}_c, \mathcal{E}_c, \mathbf{W}_c)$ , with vertices  $\mathcal{V}_c = \{1, \dots, n\}$ , edges  $\mathcal{E}_c \subseteq \mathcal{V}_c \times \mathcal{V}_c$  and weight matrix  $\mathbf{W}_c$ , for the rows of  $\mathbf{X}$ . One can thus assume bandlimitedness for the rows of  $\mathbf{X}$  with respect to the corresponding Laplacian  $\mathbf{L}_c$  [53], or simply that the rows of  $\mathbf{X}$  are smooth with respect to  $\mathbf{L}_c$  [52].

To complete formulating the matrix completion problem, given a sampling set  $\Omega = \{(i, j) \mid i \in \{1, \dots, N_r\}, j \in \{1, \dots, N_c\}\}$ , denote by  $\mathbf{A}_\Omega$  the *sampling matrix*:

$$[\mathbf{A}_\Omega]_{ij} = \begin{cases} 1, & \text{if } (i, j) \in \Omega; \\ 0, & \text{otherwise.} \end{cases} \quad (45)$$

We can now formulate the matrix completion problem with *double graph Laplacian regularization* (DGLR) as follows [54]:

$$\min_{\mathbf{X}} f(\mathbf{X}) = \frac{1}{2} \|\mathbf{A}_\Omega \circ (\mathbf{X} - \mathbf{Y})\|_F^2 + \frac{\alpha}{2} \text{Tr}(\mathbf{X}^\top \mathbf{L}_r \mathbf{X}) + \frac{\beta}{2} \text{Tr}(\mathbf{X} \mathbf{L}_c \mathbf{X}^\top) \quad (46)$$

where  $\alpha$  and  $\beta$  are weight parameters.

To solve the unconstrained QP problem (46), one can take the derivative with respect to  $\mathbf{X}$ , set it to 0, and solve for  $\mathbf{X}$ , resulting in a system of linear equations for unknown vectorized  $\text{vec}(\mathbf{X}^*)$ :

$$\left( \tilde{\mathbf{A}}_\Omega + \alpha \mathbf{I}_n \otimes \mathbf{L}_r + \beta \mathbf{L}_c \otimes \mathbf{I}_m \right) \text{vec}(\mathbf{X}^*) = \text{vec}(\mathbf{A}_\Omega \circ \mathbf{Y}) \quad (47)$$

where  $\tilde{\mathbf{A}}_\Omega = \text{diag}(\text{vec}(\mathbf{A}_\Omega))$ ,  $\text{vec}(\cdot)$  means a vector form of a matrix by stacking its columns, and  $\text{diag}(\cdot)$  creates a diagonal matrix with input vector as its diagonal elements. A solution to (47) can be efficiently solved using *conjugate gradient* (CG) [55].

In practice, often the available observed entries  $\mathbf{A}_\Omega \circ \mathbf{Y}$  in a matrix  $\mathbf{X}$  are not provided *a priori*, but must be actively sampled first. The problem of how to best choose matrix entries for later completion give a sampling budget is called *active matrix completion* [56], [57]. Extending sampling algorithms for signals in single graphs as discussed in earlier sections, authors in [53], [54] propose sampling algorithms to select matrix entries, assuming that the target signal  $\mathbf{X}$  is bandlimited or smooth over both row and column graphs, respectively. In a nutshell, [53] first select rows and columns separately based on bandlimited assumptions on row and column graphs, then choose matrix entries that are indexed by the selected rows and columns. In contrast, [54] greedily select one matrix entry at a time by considering the row and column graph smoothness alternately, where each greedy selection seeks to maximize the smallest eigenvalue of the coefficient matrix in (47)—the



E-optimality criterion. In Fig. 7, we see an example of a low-rank matrix, and sampling performance (in root mean squared error (RMSE)) of [53] (BL) under different bandwidth assumptions for row and column graphs and [54] (IGCS). We see that BL and IGCS perform comparably for large sample budget, but BL is sensitive to the assumed row and column graph bandwidths.

### C. Active Learning / Manifold Landmarking

In a *semi-supervised learning* (SSL) scenario [58], only partial labels (e.g., 0 or 1 in a binary classification task) on a subset of data are available as observations, and labels on the rest of the data need to be inferred or interpolated. Among many approaches, graph-based methods [59]–[61] model each datum as a node in a graph, connected to other nodes via undirected edges, with weights that reflect pairwise distances in a high-dimensional feature space. SSL thus translates to a signal interpolation problem in the graph signal domain. The problem of pre-selecting data for labelling to optimize subsequent SSL performance is the *active learning* problem [35], [62]–[64], which given a constructed similarity graph that connects individual data of interest, can be viewed as a sampling set selection problem [34]. More recent fast methods such as [16] that circumvent eigen-decomposition can further improve execution speed for large graphs.

*Manifold landmarking* [65]–[68] is more general than active learning, aiming to select representative landmarks (samples) on a low-dimensional manifold to label and improve subsequent learning results. It involves a similarity matrix (called alignment matrix in [68]) defined on a  $K$ -nearest-neighbor graph connecting data, such as the Laplacian matrix in *Laplacian Eigenmap* [69], and an alignment matrix in *locally linear embedding* [70] and *local tangent space alignment* [71]. Surprisingly, recent algorithms like [65], [68] that select samples based on Gershgorin circle theorem to minimize the condition number of the resulting submatrix bear strong similarity to graph sampling algorithms like [16], which performs graph sampling on kernel  $\lambda$ . It is thus conceivable that graph sampling algorithms can be adapted for manifold landmarking to improve targeted regression and classification performance [68].

## VI. CLOSING REMARKS

In this article, we overview sampling on graphs from theory to applications. The graph sampling framework is similar to sampling for standard signals, however, its realization is completely different due to the irregular nature of the graph domain. Current methods have found several interesting applications. At the same time, the following issues, both theoretical and practical aspects, are still open:

- Interconnection between vertex and spectral representations of sampling: As shown in Section III-C, two definitions can be possible for graph signal sampling. Can these sampling approaches be described in a more unified way beyond a few known special cases? This may lead to a more intuitive understanding of graph signal sampling.
- Studies beyond bandlimited graph signals: Most studies in graph signal sampling are based on sampling and reconstruction of bandlimited (or smooth) graph signals. However, as shown in Section II-B, sampling methods beyond the bandlimited setting have been studied in standard sampling. Investigating GSP systems beyond the bandlimited assumption will be beneficial for many practical applications since real data are often not bandlimited. Such examples include generalized graph sampling [22] and PGS sampling [7], [8], [72].
- Fast and efficient deterministic sampling: Eigen-decomposition-free methods are a current trend for graph signal sampling as seen in Section IV-B, but their computational complexities are still high compared to random methods. Furthermore, current deterministic approaches are mostly based on greedy sampling. A few attempts like prescreening or a combination with random selection have been presented so far [41], [73]. Faster deterministic graph sampling methods are required which will be tractable for graphs with millions and even billions of nodes.
- Fast and distributed reconstruction: Similar to sampling, the reconstruction step also requires an eigen-decomposition-free interpolation algorithm. Such an algorithm is expected to be implemented in a distributed manner. While fast filtering methods have been studied as briefly introduced in Section III, fast and more accurate interpolation methods of signals on a graph are still required.



- Applications: Some direct applications of graph signal sampling have been introduced in Section V. Note that sampling itself is ubiquitous in signal processing and machine learning: many applications can apply graph signal sampling as their important ingredients. For example, graph neural networks and point cloud processing are potential areas of application because it is often convenient to treat available data as signals on a structured graph. Continued discussions with domain experts in different areas would facilitate applications of graph sampling theory and algorithms to the wider field of data science.

## REFERENCES

- [1] Y. C. Eldar, *Sampling theory: Beyond bandlimited systems*. Cambridge, U.K.: Cambridge University Press, 2015.
- [2] Y. C. Eldar and T. Michaeli, “Beyond bandlimited sampling,” *IEEE Signal Process. Mag.*, vol. 26, no. 3, pp. 48–68, May 2009.
- [3] D. I. Shuman, S. K. Narang, P. Frossard, A. Ortega, and P. Vandergheynst, “The emerging field of signal processing on graphs: Extending high-dimensional data analysis to networks and other irregular domains,” *IEEE Signal Process. Mag.*, vol. 30, no. 3, pp. 83–98, Oct. 2013.
- [4] A. Ortega, P. Frossard, J. Kovačević, J. M. F. Moura, and P. Vandergheynst, “Graph signal processing: Overview, challenges, and applications,” *Proc. IEEE*, vol. 106, no. 5, pp. 808–828, May 2018.
- [5] A. Sandryhaila and J. M. F. Moura, “Big data analysis with signal processing on graphs: Representation and processing of massive data sets with irregular structure,” *IEEE Signal Process. Mag.*, vol. 31, no. 5, pp. 80–90, 2014.
- [6] G. Cheung, E. Magli, Y. Tanaka, and M. Ng, “Graph spectral image processing,” *Proc. IEEE*, vol. 106, no. 5, pp. 907–930, May 2018.
- [7] Y. Tanaka and Y. C. Eldar, “Generalized sampling on graphs with a subspace prior,” in *Proc. International Conference on Sampling Theory and Applications (SampTA)*, 2019.
- [8] —, “Generalized sampling on graphs with subspace and smoothness priors,” *arXiv preprint arXiv:1905.04441*, 2019.
- [9] S. Chen, R. Varma, A. Sandryhaila, and J. Kovačević, “Discrete signal processing on graphs: Sampling theory,” *IEEE Trans. Signal Process.*, vol. 63, no. 24, pp. 6510–6523, Dec. 2015.
- [10] I. Pesenson, “Sampling in Paley–Wiener spaces on combinatorial graphs,” *Transactions of the American Mathematical Society*, vol. 360, no. 10, pp. 5603–5627, 2008.
- [11] A. Anis, A. Gadde, and A. Ortega, “Efficient sampling set selection for bandlimited graph signals using graph spectral proxies,” *IEEE Trans. Signal Process.*, vol. 64, no. 14, pp. 3775–3789, Jul. 2016.
- [12] A. G. Marques, S. Segarra, G. Leus, and A. Ribeiro, “Sampling of graph signals with successive local aggregations,” *IEEE Trans. Signal Process.*, vol. 64, no. 7, pp. 1832–1843, 2016.
- [13] A. Sakiyama, Y. Tanaka, T. Tanaka, and A. Ortega, “Eigendecomposition-free sampling set selection for graph signals,” *IEEE Trans. Signal Process.*, vol. 67, no. 10, pp. 2679–2692, May 2019.
- [14] Y. Tanaka, “Spectral domain sampling of graph signals,” *IEEE Trans. Signal Process.*, vol. 66, no. 14, pp. 3752–3767, Jul. 2018.
- [15] M. Tsitsvero, S. Barbarossa, and P. Di Lorenzo, “Signals on graphs: Uncertainty principle and sampling,” *IEEE Trans. Signal Process.*, vol. 64, no. 18, pp. 4845–4860, Sep. 2016.
- [16] Y. Bai, F. Wang, G. Cheung, Y. Nakatsukasa, and W. Gao, “Fast graph sampling set selection using Gershgorin disc alignment,” *IEEE Trans. Signal Process.*, Mar. 2020, accepted.
- [17] P. D. Lorenzo, S. Barbarossa, and P. Banelli, “Sampling and recovery of graph signals,” in *Cooperative and Graph Signal Processing*. Elsevier, 2018, pp. 261–282.
- [18] J. A. Deri and J. M. F. Moura, “Spectral projector-based graph Fourier transforms,” *IEEE J. Sel. Topics Signal Process.*, vol. 11, no. 6, pp. 785–795, Sep. 2017.
- [19] B. Girault, A. Ortega, and S. S. Narayanan, “Irregularity-aware graph Fourier transforms,” *IEEE Trans. Signal Process.*, vol. 66, no. 21, pp. 5746–5761, Nov. 2018.
- [20] L. Le Magoarou, R. Gribonval, and N. Tremblay, “Approximate fast graph fourier transforms via multilayer sparse approximations,” *IEEE Trans. Signal Inf. Process. Netw.*, vol. 4, no. 2, pp. 407–420, Jun. 2018.
- [21] K.-S. Lu and A. Ortega, “Fast graph fourier transforms based on graph symmetry and bipartition,” *IEEE Trans. Signal Process.*, vol. 67, no. 18, pp. 4855–4869, Sep. 2019.
- [22] S. P. Chepuri, Y. C. Eldar, and G. Leus, “Graph sampling with and without input priors,” in *Proc. IEEE Int. Conf. Acoust., Speech and Signal Process. (ICASSP)*, 2018, pp. 4564–4568.
- [23] S. Chen, R. Varma, A. Singh, and J. Kovačević, “Representations of piecewise smooth signals on graphs,” in *Proc. IEEE Int. Conf. Acous., Speech and Signal Process. (ICASSP)*, 2016, pp. 6370–6374.
- [24] D. Valsesia, G. Fracastoro, and E. Magli, “Sampling of graph signals via randomized local aggregations,” *IEEE Trans. Signal Inf. Process. Netw.*, vol. 5, no. 2, pp. 348–359, Sep. 2018.
- [25] S. K. Narang and A. Ortega, “Compact support biorthogonal wavelet filterbanks for arbitrary undirected graphs,” *IEEE Trans. Signal Process.*, vol. 61, no. 19, pp. 4673–4685, Oct. 2013.
- [26] A. Sakiyama, K. Watanabe, Y. Tanaka, and A. Ortega, “Two-channel critically-sampled graph filter banks with spectral domain sampling,” *IEEE Trans. Signal Process.*, vol. 67, no. 6, pp. 1447–1460, Mar. 2019.
- [27] M. Vetterli, J. Kovačević, and V. K. Goyal, *Foundations of Signal Processing*. Cambridge, U.K.: Cambridge University Press, 2014.

- [28] Y. C. Eldar and G. Kutyniok, *Compressed Sensing: Theory and Applications*. Cambridge, U.K.: Cambridge university press, 2012.
- [29] S. K. Narang, A. Gadde, and A. Ortega, "Signal processing techniques for interpolation in graph structured data," in *Proc. IEEE Int. Conf. Acous., Speech and Signal Process. (ICASSP)*, 2013, pp. 5445–5449.
- [30] S. K. Narang, A. Gadde, E. Sanou, and A. Ortega, "Localized iterative methods for interpolation in graph structured data," in *Proc. IEEE Global Conf. Signal Inf. Process. (GlobalSIP)*, 2013.
- [31] Y. Yazaki, Y. Tanaka, and S. H. Chan, "Interpolation and denoising of graph signals using plug-and-play admm," in *Proc. Int. Conf. Acoust. Speech Signal Process. (ICASSP)*, 2019, pp. 5431–5435.
- [32] S. Ono, I. Yamada, and I. Kumazawa, "Total generalized variation for graph signals," in *Proc. IEEE Int. Conf. Acoust. Speech, Signal Process.*, 2015, pp. 5456–5460.
- [33] A. Heimowitz and Y. C. Eldar, "Smooth graph signal interpolation for big data," *arXiv preprint arXiv:1806.03174*, 2018.
- [34] A. Anis, A. Gadde, and A. Ortega, "Towards a sampling theorem for signals on arbitrary graphs," in *Proc. IEEE Int. Conf. Acoust. Speech, Signal Process.*, 2014, pp. 3864–3868.
- [35] A. Gadde, A. Anis, and A. Ortega, "Active semi-supervised learning using sampling theory for graph signals," in *Proc. 20th ACM SIGKDD Int. Conf. Knowl. Discov. Data Min.*, 2014, pp. 492–501.
- [36] A. Gadde and A. Ortega, "A probabilistic interpretation of sampling theory of graph signals," in *Proc. IEEE Conf. Acoust. Speech, Signal Process.*, 2015, pp. 3257–3261.
- [37] H. Shomorony and A. S. Avestimehr, "Sampling large data on graphs," in *Proc. IEEE Global Conf. Signal Inf. Process. (GlobalSIP)*, 2014, pp. 933–936.
- [38] G. Puy, N. Tremblay, R. Gribonval, and P. Vandergheynst, "Random sampling of bandlimited signals on graphs," *Applied and Computational Harmonic Analysis*, vol. 44, no. 2, pp. 446–475, Mar. 2018.
- [39] N. Perraudin, B. Ricaud, D. I. Shuman, and P. Vandergheynst, "Global and local uncertainty principles for signals on graphs," *APSIPA Transactions on Signal and Information Processing*, vol. 7, p. e3, 2018.
- [40] S. Boyd and L. Vandenberghe, *Convex optimization*. Cambridge, U.K.: Cambridge university press, 2009.
- [41] A. Jayawant and A. Ortega, "A distance-based formulation for sampling signals on graphs," in *Proc. Int. Conf. Acoust. Speech, Signal Process. (ICASSP)*, 2018, pp. 6318–6322.
- [42] F. Wang, G. Cheung, and Y. Wang, "Low-complexity graph sampling with noise and signal reconstruction via neumann series," *IEEE Trans. Signal Process.*, vol. 67, no. 21, pp. 5511–5526, 2019.
- [43] A. Krause, A. Singh, and C. Guestrin, "Near-optimal sensor placements in Gaussian processes: Theory, efficient algorithms and empirical studies," *Journal of Machine Learning Research*, vol. 9, pp. 235–284, 2008.
- [44] S. Shekkizhar and A. Ortega, "Efficient graph construction for image representation," *arXiv preprint arXiv:2002.06662*, 2020.
- [45] B. Girault and A. Ortega, "What's in a frequency: new tools for graph fourier transform visualization," *arXiv preprint arXiv:1903.08827*, 2019.
- [46] J. Ranieri, A. Chebira, and M. Vetterli, "Near-optimal sensor placement for linear inverse problems," *IEEE Trans. Signal Process.*, vol. 62, no. 5, pp. 1135–1146, 2014.
- [47] H. Jamali-Rad, A. Simonetto, X. Ma, and G. Leus, "Distributed sparsity aware sensor selection," *IEEE Transactions on Signal Processing*, vol. 63, no. 22, pp. 5951–5964, 2015.
- [48] C. Jiang, Y. C. Soh, and H. Li, "Sensor placement by maximal projection on minimum eigenspace for linear inverse problems," *IEEE Trans. Signal Process.*, vol. 64, no. 21, pp. 5595–5610, 2016.
- [49] A. Sakiyama, Y. Tanaka, T. Tanaka, and A. Ortega, "Efficient sensor position selection using graph signal sampling theory," in *Proc. IEEE Int. Conf. Acoust., Speech, Signal Process. (ICASSP)*, Shanghai, China, March 2016, pp. 6225–6229.
- [50] E. Candes and Y. Plan, "Matrix completion with noise," *Proc. IEEE*, vol. 98, no. 6, pp. 925–936, 2010.
- [51] Y. Chi, "Low-rank matrix completion," *IEEE Signal Process. Mag.*, vol. 35, no. 5, pp. 178–181, 2018.
- [52] V. Kalofolias, X. Bresson, M. Bronstein, and P. Vandergheynst, "Matrix completion on graphs," *arXiv preprint arXiv:1408.1717*, 2014.
- [53] G. Ortiz-Jimenez, M. Coutino, S. Chepuri, and G. Leus, "Sparse sampling for inverse problems with tensors," in *IEEE Transactions on Signal Processing*, vol. 67, no.12, June 2019, pp. 3272–3286.
- [54] F. Wang, Y. Wang, G. Cheung, and C. Yang, "Graph sampling for matrix completion using recurrent Gershgorin disc shift," *arXiv preprint arXiv:1906.01087*, 2019.
- [55] G. H. Golub and D. P. OLeary, "Some history of the conjugate gradient and lanczos algorithms: 1948–1976," *SIAM Rev.*, vol. 31, no. 1, pp. 50–102, 1989.
- [56] S. Chakraborty, J. Zhou, V. Balasubramanian, S. Panchanathan, I. Davidson, and J. Ye, "Active matrix completion," in *Proc. IEEE Int. Conf. Data Mining (ICDM)*, Dallas, TX, December 2013, pp. 81–90.
- [57] A. Krishnamurthy and A. Singh, "Low-rank matrix and tensor completion via adaptive sampling," *Proc. Neural Information Processing Systems (NIPS)*, vol. 98, no. 6, pp. 836–844, 2013.
- [58] B. Settles, "Active learning literature survey," University of Wisconsin-Madison Department of Computer Sciences, Tech. Rep., 2009.
- [59] M. Belkin, I. Matveeva, and P. Niyogi, "Regularization and semi-supervised learning on large graphs," in *Proc. Int. Conf. Computational Learning Theory (COLT)*, vol. 3120, 2004, pp. 624–663.
- [60] D. Shuman, M. Faraji, and P. Vandergheynst, "Semi-supervised learning with spectral graph wavelets," in *Proc. Int. Conf. Sampling Theory and Applications (SampTA)*, May 2004.
- [61] G. Cheung, W.-T. Su, Y. Mao, and C.-W. Lin, "Robust semisupervised graph classifier learning with negative edge weights," *IEEE Trans. Signal Inf. Process. Netw.*, vol. 4, no. 4, pp. 712–726, Dec. 2018.

- [62] A. Guilloery and J. Bilmes, “Label selection on graphs,” in *Proc. Advances in Neural Information Processing Systems (NIPS)*, December 2009, pp. 691–699.
- [63] P.-Y. Chen and D. Wei, “On the supermodularity of active graph-based semi-supervised learning with stieltjes matrix regularization,” in *Proc. IEEE Int. Conf. Acoust., Speech, Signal Process. (ICASSP)*, 2018, pp. 2801–2805.
- [64] A. Anis, A. El Gamal, A. S. Avestimehr, and A. Ortega, “A sampling theory perspective of graph-based semi-supervised learning,” *IEEE Transactions on Information Theory*, vol. 65, no. 4, pp. 2322–2342, 2018.
- [65] H. Xu, H. Zha, R.-C. Li, and M. A. Davenport, “Active manifold learning via gershgorin circle guided sample selection,” in *Twenty-Ninth AAAI Conference on Artificial Intelligence*, 2015.
- [66] J. Silva, J. Marques, and J. Lemos, “Selecting landmark points for sparse manifold learning,” in *Proc. Advances in Neural Information Processing Systems (NIPS)*, 2006, pp. 1241–1248.
- [67] C. Wachinger and P. Golland, “Diverse landmark sampling from determinantal point processes for scalable manifold learning,” *arXiv preprint arXiv:1503.03506*, 2015.
- [68] H. Xu, L. Yu, M. A. Davenport, and H. Zha, “A unified framework for manifold landmarking,” *IEEE Transactions on Signal Processing*, vol. 66, no. 21, pp. 5563–5576, 2018.
- [69] P. Vepakomma and A. Elgammal, “A fast algorithm for manifold learning by posing it as a symmetric diagonally dominant linear system,” *Applied and Computational Harmonic Analysis*, vol. 40, no. 3, pp. 622–628, 2016.
- [70] S. T. Roweis and L. K. Saul, “Nonlinear dimensionality reduction by locally linear embedding,” *Science*, vol. 290, no. 5500, pp. 2323–2326, 2000.
- [71] Z. Zhang and H. Zha, “Principal manifolds and nonlinear dimensionality reduction via tangent space alignment,” *SIAM J. Sci. Comput.*, vol. 26, no. 1, pp. 313–338, 2004.
- [72] J. Hara, Y. Tanaka, and Y. C. Eldar, “Generalized graph spectral sampling with stochastic priors,” in *Proc. IEEE Int. Conf. Acoust. Speech, Signal Process. (ICASSP)*, 2020, to be presented.
- [73] S. Chen, D. Tian, C. Feng, A. Vetro, and J. Kovačević, “Fast resampling of three-dimensional point clouds via graphs,” *IEEE Transactions on Signal Processing*, vol. 66, no. 3, pp. 666–681, 2017.